Quality-Weighted Thermophysical Property Database and Uncertainty Quantification for Molten Salts

Hanuel Park[a], Chaehyun Kim[a], Dongwoo Lee[a], Woosung Joo[a], Chanyeong Choi[a], Yejun Han[a], Junsu Bang[a], Yong Hoon Jeong[a*]

[a] *Department of Nuclear and Quantum Engineering, Korea Advanced Institute of Science and Technology, 291 Daehak-ro, Yuseong-gu, Daejeon 305-701, the Republic of Korea*

[*] *Corresponding author: jeongyh@kaist.ac.kr*

Keywords : molten salt reactor, thermophysical properties, data quality, uncertainty quantification, composition interpolation

1. Introduction

Reliable thermophysical property correlations are required for thermal-hydraulic design and safety analysis of molten salt reactor (MSR) systems. Density, viscosity, specific heat capacity, and thermal conductivity influence buoyancy-driven flow, hydraulic resistance, heat transfer, and transient heat removal. Uncertainty in these properties therefore propagates directly into predicted system behavior under normal operating and accident conditions.

Thermophysical property measurements for molten salts have been reported over a wide range of temperatures and compositions using different experimental techniques and correlation forms. The available studies also differ in reported measurement uncertainty, fitting error, number of experimental data points, and agreement with independent measurements. Direct use of a single literature correlation may therefore depend strongly on source selection, whereas unweighted averaging disregards differences in the supporting experimental evidence. A database intended for uncertainty-informed safety analysis should retain these differences and provide a quantitative basis for combining the available information.

Several studies have addressed different aspects of this problem. Sohal et al. [1] compiled an engineering database of candidate molten salts, including FLiBe and FLiNaK, and identified limitations in available correlations for key thermophysical properties. More recent work at Oak Ridge National Laboratory by Ezell et al. [2] focused on recharacterizing MSR-relevant salts, including FLiNaK, with particular attention to measurement-method validation and uncertainty quantification for density, viscosity, specific heat capacity, and thermal conductivity. Experimental coverage has also expanded to fuel-bearing compositions; Ivory et al. [3] reported density and specific heat capacity measurements for UF_4-FLiNaK together with an unfueled FLiNaK baseline. The practical importance of correlation selection was demonstrated by Freile and Kimber [4], who showed that alternative FLiNaK thermophysical-property correlations can produce appreciable differences in CFD-predicted heat-transfer behavior.

These studies demonstrate both the continuing need to improve molten-salt property data and the sensitivity of thermal-hydraulic predictions to the correlations selected. However, literature compilation, new property measurements, and sensitivity assessment have generally been treated as separate tasks. A systematic procedure is still needed to screen multiple source correlations, quantify their relative quality, construct representative correlations without relying on a single selected source, and propagate the associated uncertainty when properties are estimated at unmeasured compositions.

In this study, a literature-based thermophysical property database is developed for representative fluoride- and chloride-based molten salts, including FLiBe, FLiNaK, NaF–KF–UF_4, $MgCl_2$–KCl–NaCl, and related binary and ternary systems relevant to MSR and heat-transfer applications. The database records the reported correlation, salt composition, applicable temperature range, number of experimental data points, measurement uncertainty, fitting error, and source information. Throughout this paper, a source correlation denotes a literature correlation together with the experimental data and metadata used to support that correlation.

The relative quality of each source correlation is evaluated using three quantitative criteria: reported error, number of experimental data points, and inter-study consistency. These criteria are combined into a quality score and a corresponding relative weight. The coefficients used to combine the criteria are not fixed a priori but are treated as adjustable parameters to be determined through optimization.

Property prediction is performed in two stages. First, source correlations available at the same measured composition are combined according to their quality weights to obtain a representative correlation. Second, properties at unmeasured compositions are estimated by interpolation between the representative correlations. All evaluations are restricted to the originally reported temperature ranges; temperature extrapolation is not used. Reported uncertainty and fitting-error measures are converted to a common standard-uncertainty basis and propagated through the weighting and interpolation procedures. This approach provides representative property estimates together with uncertainty intervals for

subsequent uncertainty-informed thermal-hydraulic and safety analyses.

To implement the methodology in a reproducible computational form, the screened literature data were encoded in structured JSON files and a Python program was developed to execute the full calculation from database query to uncertainty evaluation. The implementation is demonstrated using FLiBe density data and a fixed-composition KCl–$MgCl_2$ thermal-conductivity case. The examples first present five source density correlations at measured FLiBe compositions, then demonstrate quality-weighted integration of multiple KCl–$MgCl_2$ thermal-conductivity source correlations at a single measured composition, and finally demonstrate prediction of FLiBe density and its uncertainty at an unmeasured composition. These examples illustrate the end-to-end operation of the database and analysis procedure.

2. Database Construction and Computational Implementation

2.1 Literature Data Collection and Screening

Thermophysical property data and correlations were collected from the literature and classified by salt composition and property. The target systems were grouped broadly into fluoride- and chloride-based salts according to their relevance to MSR primary systems, secondary heat-transfer systems, and fuel-cycle applications.

For fluoride-based salts, FLiBe (LiF–BeF_2) was included as a representative salt for thermal-spectrum reactor concepts, and FLiNaK (LiF–NaF–KF) was included because of its extensive use in heat-transfer studies and its relatively low melting point. NaF–KF–UF_4 was also considered to represent fuel salts containing dissolved uranium species and to capture composition-dependent property changes associated with fuel-bearing components.

For chloride-based salts, $MgCl_2$–KCl–NaCl was selected as a primary system because of its relevance to primary and secondary coolant applications and the availability of data over a broad composition range. Literature data for $MgCl_2$–NaCl, KCl–$MgCl_2$, and ternary $MgCl_2$–KCl–NaCl were treated within a common composition space. The two binary systems correspond to limiting compositions of the ternary system when the mole fraction of KCl or NaCl is zero, respectively. Treating them together permits consistent evaluation across the available composition domain.

The database covers four thermophysical properties: density, viscosity, specific heat capacity, and thermal conductivity. Density affects buoyancy and natural circulation and can influence reactivity through temperature-dependent changes in fuel- or coolant-salt density. Viscosity governs hydraulic resistance and pressure loss and is directly related to pumping requirements. Specific heat capacity and thermal conductivity determine heat storage, heat transfer, and the transient thermal response of the salt and are therefore important to fission- and decay-heat removal analyses.

More than 50 literature sources were initially reviewed. Duplicate datasets derived from the same underlying measurements and datasets with excessively large reported measurement uncertainty or fitting error were removed during screening, leaving 32 literature sources represented in the final database. The retained literature includes experimental studies and technical reports from national laboratories, historical measurements associated with the Molten Salt Reactor Experiment and related Oak Ridge National Laboratory programs, and more recent peer-reviewed studies. Together, these sources cover both historical datasets and later measurements and reassessments reflecting advances in experimental techniques, recognition of instrumental limitations or sample loss, and the growing body of data for chloride-based salt systems.

For multicomponent salts, thermophysical properties may vary with both temperature and composition. This dependence is particularly relevant to fuel salts containing uranium species, whose concentrations can change during reactor operation. Restricting the database to a single nominal or eutectic composition would therefore be insufficient for composition-dependent property prediction. Experimental data and source correlations covering multiple binary and ternary compositions were collected where available. The number of available correlations and their corresponding source literature for each salt and property are summarized in Table I.

Table I: Summary of thermophysical property correlations and data sources for selected molten salts

Salt system	Density	Viscosity	Specific Heat Capacity	Thermal Conductivity
FLiBe	4 [5, 6, 7, 8]	7 [6, 8, 9, 10, 11, 12, 13]	3 [14, 15, 16]	1 [9]
FLiNaK	4 [17, 18, 19, 20]	4 [12, 17, 20, 21]	2 [22, 23]	1 [24]
NaF–KF–UF_4	3 [25, 26, 27]	4 [12, 26, 28]	2 [26, 29]	1 [30]
$MgCl_2$–KCl–NaCl	6 [31, 32, 33, 34, 35, 36]	4 [32, 34, 35, 36]	4 [23, 32, 34, 36]	4 [32, 34, 35, 36]

Note: Numbers indicate the number of available correlations. Bracketed citations identify the corresponding source literature. A publication may provide more than one correlation or may be cited for more than one property.

2.2 JSON Database and Python Implementation

Following literature screening, the retained source correlations and their associated metadata were organized as structured JSON files. For each source correlation, the database stores the information required for identification and evaluation, including the salt system and composition, thermophysical property, applicable temperature range, correlation definition, number of supporting experimental data points, reported measurement uncertainty or fitting error, and source

information. Maintaining these entries in a machine-readable format allows the same database to be queried consistently across different salts, properties, temperatures, and compositions while preserving the provenance of each source correlation.

A Python program was developed to read the JSON database and perform the procedures described in Sections 3 and 4. For a specified salt and thermophysical property, the program identifies the applicable source correlations, evaluates the quality criteria and relative weights, constructs quality-weighted representative correlations at measured compositions, performs composition interpolation when a target composition is not directly available, and propagates the associated standard uncertainties. The same implementation is used to generate the demonstration results presented in Section 5. The database and analysis program are kept separate so that additional literature correlations can be incorporated without changing the calculation procedure.

3. Data Integration and Quality Weighting

The collected source correlations were integrated into a common database and compared within each salt–property group. Because the supporting experiments differ in reported error, number of measurements, and agreement with independent studies, equal weighting was not assumed. Three criterion scores were evaluated for each source correlation: an error-based score, a data-point score, and an inter-study consistency score. These scores were then combined to obtain an overall quality score and relative quality weight.

3.1 Error-Based Quality Score

The first criterion evaluates the quantitative error reported for each source correlation. Measurement uncertainty and fitting error were recorded separately because they describe different aspects of the source data. Measurement uncertainty characterizes the experimental measurement, whereas fitting error describes the deviation between a reported correlation and the measurements used to develop or assess it. Source correlations for which neither quantity could be identified were excluded from the quantitative quality-weighting procedure.

Reported uncertainty and fitting-error measures can be expressed in different forms across the literature. Before quality scoring and subsequent uncertainty propagation, the reported quantities were converted to a common standard-uncertainty basis. For each salt–property group, the converted error magnitude was then normalized so that a smaller value received a higher score:

$$S_{E,i} = \frac{E_{\max} - E_i}{E_{\max} - E_{\min}} \tag{1}$$

where the error magnitude corresponds to either the measurement-uncertainty or fitting-error measure after conversion to the common basis. The minimum and maximum values are evaluated within the same salt–property group. The smallest reported error receives a score of 1 and the largest a score of 0. If the maximum and minimum values are identical, the score is set to 0.5 because the available data do not support a relative distinction.

The normalized measurement-uncertainty and fitting-error scores are combined as

$$S_{\mathrm{err},i} = \alpha_{\mathrm{exp}} S_{\mathrm{exp},i} + \alpha_{\mathrm{fit}} S_{\mathrm{fit},i} \tag{2}$$

where $\alpha_{\mathrm{exp}} + \alpha_{\mathrm{fit}} = 1,\ \alpha_{\mathrm{exp}} \geq 0,\ \alpha_{\mathrm{fit}} \geq 0.$

When only one of the two error measures is available, its normalized score is used directly. The two coefficients are treated as adjustable parameters and are determined independently from the weights assigned to the three major quality criteria. The resulting error-based score is a relative quality metric and is not itself used as a statistical uncertainty.

Example of Error-Based Normalization. As an illustrative case, consider four independent density correlations for the same molten salt with fitting errors of 0.8%, 1.5%, 2.5%, and 4.0%. The corresponding normalized scores are shown in Table II.

Table II: Example of error-based normalization

Source correlation	Reported fitting error	Error score
A	0.8%	1.000
B	1.5%	0.781
C	2.5%	0.469
D	4.0%	0.000

Correlation A receives the highest score because it has the smallest reported fitting error, whereas correlation D receives the lowest score. The score only ranks the reported error within the same salt–property group and does not imply that a low-scoring correlation is experimentally invalid.

3.2 Data-Point-Based Quality Score

The second criterion accounts for the amount of experimental data supporting each source correlation. The number of experimental data points used to develop or validate source correlation i is denoted by N_i. Because a linear dependence on N_i would give excessive influence to very large datasets, a logarithmic transformation is used:

$$S_{N,i} = \frac{\ln(1+N_i)}{\ln(1+N_{\max})} \tag{3}$$

where the denominator uses the largest reported number of experimental data points within the same salt–property group. The logarithmic form introduces diminishing returns as the number of points increases; an increase from 10 to 100 points is given greater relative importance than an increase from 1,000 to 1,090 points.

The data-point score reflects the amount of experimental data supporting a correlation rather than its experimental accuracy. Accuracy is evaluated separately through the error-based criterion. If the number of supporting data points is not explicitly reported, the data-point criterion is treated as unavailable and is handled through weight renormalization in Section 3.4 rather than being assigned an estimated value.

3.3 Inter-Study Consistency

The third criterion measures agreement with independent source correlations for the same salt and thermophysical property. Small measurement uncertainty or fitting error within an individual study does not exclude the possibility of systematic differences between experimental campaigns; inter-study agreement is therefore evaluated separately.

For source correlations i and j, both correlations are evaluated over their common temperature–composition domain. At each common evaluation condition k, the symmetric relative deviation is defined as

$$d_{ij,k} = \frac{|y_{i,k} - y_{j,k}|}{\frac{|y_{i,k}| + |y_{j,k}|}{2}} \tag{4}$$

where y_i,k and y_j,k are the property values calculated from the two source correlations at the same condition. Using the average magnitude of the two values in the denominator gives a symmetric measure and avoids designating either source correlation as the reference.

The mean pairwise deviation for source correlation i is calculated as

$$D_i = \frac{\sum_{j \neq i} \frac{\sum_{k=1}^{K_{ij}} d_{ij,k}}{K_{ij}}}{M_i} \tag{5}$$

The inner average is taken over the common evaluation conditions for each pair of source correlations, and the outer average is taken over the independent source correlations that overlap with source correlation i. Only the overlapping temperature and composition domain is used in the comparison.

A smaller mean pairwise deviation indicates better agreement with the other available correlations. To place the consistency criterion on the same 0–1 scale as the other quality scores, the mean pairwise deviation is normalized within each salt–property group as

$$S_{\mathrm{cons},i} = \frac{D_{\max} - D_i}{D_{\max} - D_{\min}} \tag{6}$$

The source correlation with the smallest mean pairwise deviation receives a score of 1, and that with the largest deviation receives a score of 0. If the maximum and minimum mean deviations are identical, all corresponding consistency scores are set to 0.5. When no independent source correlation overlaps the applicable domain of a given source correlation, the consistency criterion is treated as unavailable and is handled as described in Section 3.4.

The consistency score describes agreement with the available literature, not absolute experimental accuracy. Differences among studies may reflect composition, impurity concentration, experimental method, or other systematic effects. The score is therefore used only as one component of the overall quality assessment.

3.4 Overall Quality Score and Relative Weight

The three criterion scores capture different aspects of the supporting evidence: reported quantitative error, amount of experimental data, and agreement with independent studies. For a source correlation for which all three criteria are available, the overall quality score is

$$Q_i = w_{\mathrm{err}} S_{\mathrm{err},i} + w_N S_{N,i} + w_{\mathrm{cons}} S_{\mathrm{cons},i} \tag{7}$$

where $w_{\mathrm{err}} + w_N + w_{\mathrm{cons}} = 1,\ \ w_{\mathrm{err}}, w_N, w_{\mathrm{cons}} \geq 0.$

The weighting coefficients are not assumed to be equal. They are treated as adjustable parameters and will be determined through optimization so that the relative influence of the three criteria can be evaluated rather than prescribed a priori. For the demonstration calculations presented in Section 5, equal weights (w_err = w_N = w_cons = 1/3) were used provisionally, while optimization of these coefficients is reserved for subsequent work.

If the data-point or consistency criterion cannot be evaluated for a source correlation, the unavailable term is omitted and the remaining criterion weights are renormalized to sum to one for that source correlation. Because source correlations lacking both measurement uncertainty and fitting error are excluded, an error-based score is always available for correlations entering the quality-weighting procedure.

The resulting quality scores are normalized within each salt–property group to obtain relative quality weights:

$$W_i = \frac{Q_i}{\sum_{j=1}^{n} Q_j} \tag{8}$$

(By definition, $\sum_{i=1}^{n} W_i = 1$.)

where n is the number of source correlations in the corresponding salt–property group. The resulting relative weight determines the contribution of a source correlation when representative property correlations are constructed. It is a quality weight, not a statistical uncertainty or a probability that a particular correlation is correct.

4. Property Prediction and Uncertainty Estimation

The quality weights obtained in Section 3 are used to construct representative thermophysical property correlations and to estimate properties at compositions without direct measurements. The calculation is

separated into two stages so that the quality assessment of the literature data does not alter the geometric dependence of composition interpolation. All evaluations remain within the originally reported temperature ranges of the source correlations; temperature extrapolation is not performed.

4.1 Quality-Weighted Representative Correlations at Measured Compositions

At a measured composition, several independent source correlations may be available for the same thermophysical property. These correlations are first combined using their quality weights. At a given temperature and measured composition, only source correlations whose reported temperature ranges include that temperature are used. Denoting this active set by $I_r(T)$, the corresponding quality weights are renormalized as

$$\omega_{i,r}(T) = \frac{w_i}{\sum_{j \in I_r(T)} w_j} \tag{9}$$

for each source correlation in the active set. The representative property at the measured composition is then

$$\overline{y}_r(T) = \sum_{i \in I_r(T)} \omega_{i,r}(T) y_i(T) \tag{10}$$

where each source term is evaluated at the specified temperature. This step accounts for differences in source quality at an experimentally investigated composition before any interpolation in composition space is performed.

Because the set of active source correlations may change at the boundaries of their reported temperature ranges, the pointwise quality-weighted property may exhibit small discontinuities. A continuous representative correlation is therefore fitted to the pointwise weighted values over the combined temperature range supported by the source correlations. The residual fitting error from this step is converted to an additional standard-uncertainty contribution and propagated as described in Section 4.3.

4.2 Prediction at Unmeasured Compositions

Properties at unmeasured compositions are estimated from the continuous representative correlations obtained in Section 4.1. For a target composition x*, the property at temperature T is expressed in general form as

$$\hat{y}(T, x^\star) = \sum_{r=1}^{R} \lambda_r(x^\star) \tilde{y}_r(T) \tag{11}$$

where R is the number of neighboring measured compositions used in the interpolation.

The composition-dependent coefficients satisfy $\lambda_r(x^\star) \geq 0, \ \sum_{r=1}^{R} \lambda_r(x^\star) = 1$.

The target composition may be represented by a single composition coordinate or by a multicomponent composition vector, depending on the salt system. The interpolation formulation is selected according to the number and distribution of the available measured compositions.

For linear interpolation between two neighboring measured compositions, the coefficients are

$$\lambda_1 = \frac{x_2 - x^\star}{x_2 - x_1}, \ \ \lambda_2 = \frac{x^\star - x_1}{x_2 - x_1} \tag{12}$$

$$\hat{y}(T, x^\star) = \lambda_1 \tilde{y}_1(T) + \lambda_2 \tilde{y}_2(T) \tag{13}$$

Composition interpolation is restricted to the domain bounded by the available measurements; composition extrapolation is not used. The source quality weights do not enter the composition-interpolation coefficients directly. Quality weighting is completed in the first stage at measured compositions, whereas the interpolation coefficients depend only on the location of the target composition relative to the measured compositions. This separation preserves the intended composition dependence of the interpolation.

4.3 Propagation of Prediction Uncertainty

Uncertainty is evaluated separately from the quality score. The quality weights control the contribution of each source correlation to the representative property, whereas uncertainty propagation quantifies uncertainty in the resulting estimate.

The reported measurement uncertainty and fitting error are converted to the common standard-uncertainty basis introduced in Section 3.1. At a given temperature, the measurement and fitting contributions are expressed as standard uncertainties in the property value. Assuming independence between these contributions, the combined standard uncertainty of source correlation i is

$$u_i^{\,2} = u_{\mathrm{meas},i}^{\,2} + u_{\mathrm{fit},i}^{\,2} \tag{14}$$

When only one of the measurement-uncertainty or fitting-error measures is available, the source-correlation uncertainty is evaluated using only the available component; no uncertainty value is imputed for the unavailable component.

At a measured composition, the standard uncertainty of the continuous representative correlation includes both the propagated uncertainty of the quality-weighted source correlations and the additional uncertainty introduced by fitting the continuous representative correlation:

$$u_r^2(T) = \sum_{i \in \mathcal{I}_r(T)} \omega_{i,r}^2(T) u_i^2(T) + u_{\mathrm{repfit},r}^2(T) \tag{15}$$

The final term represents the standard uncertainty associated with fitting the continuous representative correlation to the pointwise weighted values. This contribution is included in the composition-interpolation uncertainty through the measured-composition uncertainty defined above.

The uncertainty at an unmeasured composition is then propagated through the composition interpolation:

$$u_{\text{pred}}{}^2(T, x^\star) = \sum_{r=1}^{R} \lambda_r{}^2(x^\star) u_r{}^2(T) \qquad (16)$$

For linear interpolation between two neighboring compositions, this expression reduces to

$$u_{\text{pred}}{}^2 = \lambda_1{}^2 u_1{}^2 + \lambda_2{}^2 u_2{}^2 \qquad (17)$$

The same propagation principle is used for multicomponent interpolation with the corresponding interpolation coefficients. The formulation assumes statistical independence among the source-correlation uncertainty contributions and the additional representative-correlation fitting contribution. The resulting quantity is the combined standard uncertainty associated with the quality-weighted literature correlations, fitting of the continuous representative correlations, and interpolation in composition space.

4.4 Uncertainty Interval

The combined standard uncertainty is used to construct an approximate uncertainty interval for the predicted thermophysical property. Under a normal approximation, the two-sided 100(1−α)% uncertainty interval is

$$\text{UI}_{1-\alpha} = \left[\hat{y} - z_{1-\frac{\alpha}{2}} u_{\text{pred}}, \hat{y} + z_{1-\frac{\alpha}{2}} u_{\text{pred}}\right] \qquad (18)$$

where the interval is centered on the predicted thermophysical property, the uncertainty term is the combined standard uncertainty defined in Section 4.3, and z is the corresponding standard normal quantile. For an approximate 95% uncertainty interval,

$$z_{0.975} = 1.96,$$
$$\text{UI}_{95\%} = \left[\hat{y} - 1.96 u_{\text{pred}}, \hat{y} + 1.96 u_{\text{pred}}\right] \qquad (19)$$

This interval characterizes uncertainty in the estimated thermophysical property under the adopted uncertainty model. It is not interpreted as a statistical prediction interval for repeated future measurements. Rather, it summarizes the measurement, source-correlation fitting, and representative-correlation fitting uncertainties propagated through the quality-weighting and composition-interpolation procedures.

5. Demonstration Results

Representative calculations generated with the Python implementation are presented using FLiBe density data and a fixed-composition KCl–$MgCl_2$ thermal-conductivity case. Rather than reproducing the full database, the examples are arranged to follow the computational sequence described above: retrieval of source correlations, quality-weighted integration at a measured composition, and interpolation to an unmeasured composition.

5.1 Source FLiBe Density Correlations at Measured Compositions

Fig. 1 presents five source density correlations for the FLiBe system at different measured compositions retrieved from the JSON database. Each curve corresponds to one composition and retains its originally reported temperature range. No quality weighting or composition interpolation is applied at this stage. The figure therefore represents the direct literature inputs used by the subsequent integration procedure and provides a compact view of the available density information across the selected FLiBe compositions.

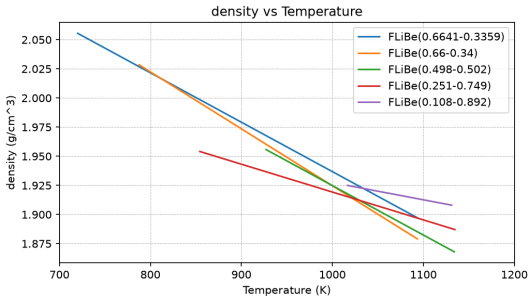

Fig. 1. Source FLiBe density correlations retrieved from the JSON database for five measured compositions

5.2 Quality-Weighted Integration at a Measured Composition

When more than one source correlation is available at the same composition, the Python program applies the procedure in Sections 3 and 4.1 to obtain a single representative correlation. The quality criteria are evaluated for the applicable source correlations, their relative quality weights are calculated, and the source predictions are combined using the normalized weights at each temperature. Measurement and fitting uncertainties from the source correlations are propagated through the weighting operation, and the additional fitting error introduced when the continuous representative correlation is fitted to the pointwise weighted values is included in the final uncertainty.
Fig. 2 provides an example of this fixed-composition integration. The pointwise quality-weighted combination of the source correlations is shown together with the continuous representative correlation fitted to those values and the corresponding uncertainty interval. Because the set of active source correlations changes at the boundaries of their reported temperature ranges, the pointwise weighted estimate exhibits small discontinuities. Fitting a continuous representative correlation removes these discontinuities over the combined supported temperature range, while introducing an additional fitting error.

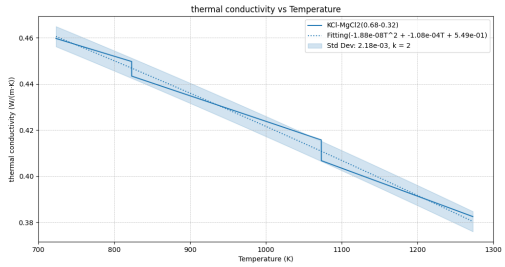

Fig. 2. Example of quality-weighted integration of multiple KCl–$MgCl_2$ thermal conductivity source correlations at a single measured composition [0.68-0.32]. The pointwise quality-weighted combination of source correlations, the fitted continuous representative correlation, and the corresponding uncertainty interval are shown.

5.3 Prediction at an Unmeasured Composition

The second stage of the calculation is demonstrated by predicting density at a FLiBe composition for which no direct source correlation is used as the target. The program first constructs the representative correlations at the surrounding measured compositions and then evaluates the target composition using the composition-interpolation coefficients defined in Section 4.2. The corresponding standard uncertainties are propagated with the same interpolation coefficients, as described in Section 4.3. Because quality weighting is completed before composition interpolation, differences in source quality affect the representative correlations at the measured compositions but do not alter the interpolation geometry.

Fig. 3 shows the resulting density correlation and uncertainty interval at the selected target composition together with the representative correlations used to perform the interpolation. This example demonstrates the complete calculation from the JSON database to a property estimate at an unmeasured composition.

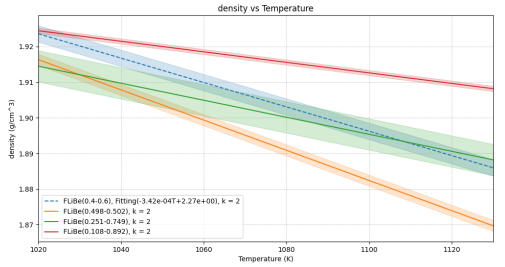

Fig. 3. Prediction of FLiBe density at an unmeasured target composition [0.4-0.6] using representative correlations at neighboring measured compositions. The predicted correlation and propagated uncertainty interval are shown together with the representative correlations used for composition interpolation.

6. Conclusions

A literature-based database and computational procedure were developed to integrate thermophysical property correlations for molten salts while retaining quantitative information on the supporting experimental evidence. More than 50 literature sources were reviewed, and 32 were retained after screening duplicate datasets and data with excessively large reported measurement uncertainty or fitting error. The retained source correlations and metadata were organized in structured JSON files, and a Python program was implemented to read the database and execute the quality assessment, weighting, composition interpolation, and uncertainty-propagation procedures.

Each source correlation is assigned a relative quality weight based on reported error, amount of experimental data, and agreement with independent studies. Multiple source correlations at a measured composition are first combined pointwise according to their quality weights and then fitted with a continuous representative correlation. The fitting uncertainty introduced in this step is included in the propagated uncertainty. Composition interpolation is subsequently performed between the representative correlations. This two-stage procedure keeps source-quality assessment separate from composition interpolation, and both temperature and composition extrapolation are excluded from the present method. Measurement uncertainty and fitting error are converted to a common standard-uncertainty basis and propagated through the same weighting and interpolation operations used for the property estimate.

The Python implementation was demonstrated using FLiBe density data and a fixed-composition KCl–$MgCl_2$ thermal-conductivity case. Five measured FLiBe compositions were used to present the source database inputs, a fixed-composition thermal-conductivity case illustrates the integration of multiple source correlations into a single continuous representative correlation with uncertainty, and an additional FLiBe case demonstrates density prediction at an unmeasured composition. These examples establish the end-to-end operation of the database and computational workflow; they are not intended as an independent validation of predictive accuracy. Optimization of the criterion-weighting coefficients, systematic validation against withheld data, and propagation of the resulting property uncertainties into reactor thermal-hydraulic and safety analyses constitute the next stages of the work.

REFERENCES

[1] M.S. Sohal, M.A. Ebner, P. Sabharwall, P. Sharpe, Engineering Database of Liquid Salt Thermophysical and Thermochemical Properties, INL/EXT-10-18297, Rev. 1, Idaho National Laboratory, Idaho Falls, ID, June 2013.
[2] N.D.B. Ezell, R.C. Gallagher, C. Agca, J.W. McMurray, Thermal Property Characterization of Molten Salt Reactor-Relevant Salts, ORNL/TM-2021/2216, Oak Ridge National Laboratory, Oak Ridge, TN, 2021. https://doi.org/10.2172/1844891.
[3] J. Ivory, A. Nielson, D. Walton, M.J. Memmott, Thermophysical property analysis of UF_4-FLiNaK molten salt: Density and heat capacity measurements, Progress in Nuclear Energy 192 (2026) 106157. https://doi.org/10.1016/j.pnucene.2025.106157.

[4] R. Freile, M. Kimber, Influence of molten salt-(FLiNaK) thermophysical properties on a heated tube using CFD RANS turbulence modeling of an experimental testbed, EPJ Nuclear Sciences & Technologies 5 (2019) 16. https://doi.org/10.1051/epjn/2019027.
[5] R. Vidrio, S. Mastromarino, E. Still, L. Chapdelaine, and R.O. Scarlat, "Density and Thermal Expansivity of Molten 2LiF–BeF2," Journal of Chemical and Engineering Data, Vol. 67, pp. 3517–3531, 2022. DOI: 10.1021/acs.jced.2c00212.
[6] S. Cantor, "Density and Viscosity of Several Molten Fluoride Mixtures," ORNL-TM-4308, Oak Ridge National Laboratory, Oak Ridge, TN, 1973. DOI: 10.2172/4419855.
[7] Oak Ridge National Laboratory, "Molten-Salt Reactor Program Quarterly Progress Report for Period Ending October 31, 1958," ORNL-2626, Oak Ridge National Laboratory, Oak Ridge, TN, 1959. DOI: 10.2172/4274257.
[8] S. Cantor, W.T. Ward, and C.T. Moynihan, "Viscosity and Density in Molten BeF2–LiF Solutions," The Journal of Chemical Physics, Vol. 50, No. 7, pp. 2874–2879, 1969. DOI: 10.1063/1.1671478.
[9] S. Cantor, J.W. Cooke, A.S. Dworkin, G.D. Robbins, R.E. Thoma, and G.M. Watson, "Physical Properties of Molten-Salt Reactor Fuel, Coolant, and Flush Salts," ORNL-TM-2316, Oak Ridge National Laboratory, Oak Ridge, TN, 1968. DOI: 10.2172/4492893.
[10] W.R. Grimes, "Reactor Chemistry Division Annual Progress Report for Period Ending December 31, 1965," ORNL-3913, Oak Ridge National Laboratory, Oak Ridge, TN, 1966. DOI: 10.2172/4547015.
[11] W.R. Grimes, "Reactor Chemistry Division Annual Progress Report for Period Ending January 31, 1964," ORNL-3591, Oak Ridge National Laboratory, Oak Ridge, TN, 1964. DOI: 10.2172/4000934.
[12] S.I. Cohen and T.N. Jones, "Viscosity Measurements on Molten Fluoride Mixtures," ORNL-2278, Oak Ridge National Laboratory, Oak Ridge, TN, 1957. DOI: 10.2172/4803933.
[13] Y. Abe, O. Kosugiyama, and A. Nagashima, "Viscosity of LiF-BeF2 Eutectic Mixture (XBeF2 = 0.328) and LiF Single Salt at Elevated Temperatures," Journal of Nuclear Materials, Vol. 99, pp. 173–183, 1981. DOI: 10.1016/0022-3115(81)90186-0.
[14] Oak Ridge National Laboratory, "Molten-Salt Reactor Program Semiannual Progress Report for Period Ending August 31, 1968," ORNL-4344, Oak Ridge National Laboratory, Oak Ridge, TN, 1969. DOI: 10.2172/4487235.
[15] W.R. Grimes, "Reactor Chemistry Division Annual Progress Report for Period Ending January 31, 1965," ORNL-3789, Oak Ridge National Laboratory, Oak Ridge, TN, 1965. DOI: 10.2172/4616564.
[16] National Bureau of Standards, "Preliminary Report on the Thermodynamic Properties of Selected Light-Element and Some Related Compounds: Supplement to NBS Reports 6297, 6484, 6645, 6928, 7093, 7192, 7437, 7587, 7796, and 8033," NBS Report 8186, U.S. Department of Commerce, Washington, DC, 1964. DOI: 10.6028/NBS.RPT.8186.
[17] J. Cibulková, M. Chrenková, R. Vasiljev, V. Kremenetsky, and E. Polyakov, "Density and Viscosity of the (LiF + NaF + KF)eut (1) + K2TaF7 (2) + Ta2O5 (3) Melts," Journal of Chemical and Engineering Data, Vol. 51, No. 3, pp. 984–987, 2006. DOI: 10.1021/je050490g.
[18] T. Munro et al., "Round Robin Measurements of Molten Salt Properties for LiF–NaF–KF and NaCl–KCl," Journal of Chemical and Engineering Data, Vol. 71, pp. 1541–1565, 2026. DOI: 10.1021/acs.jced.5c00421.
[19] R.C. Gallagher, C. Agca, N. Russell, J.W. McMurray, and N.D. Bull Ezell, "Assessment of Molten Eutectic LiF–NaF–KF Density through Experimental Determination and Semiempirical Modeling," Journal of Chemical & Engineering Data, Vol. 67, No. 6, pp. 1406–1414, 2022.
[20] M.A. Rose, E. Wu, and M.A. Williamson, "Thermophysical Property Measurements: Improved Density, Viscosity and Thermal Diffusivity Methods," ANL/CFCT-20/38, Argonne National Laboratory, Argonne, IL, 2020. DOI: 10.2172/1734862.
[21] K. Tørklep and H.A. Øye, "Viscosity of the Eutectic Lithium Fluoride-Sodium Fluoride-Potassium Fluoride Melt (FLINAK)," Journal of Chemical and Engineering Data, Vol. 25, No. 1, pp. 16–20, 1980. DOI: 10.1021/je60084a007.
[22] D.J. Rogers, T. Yoko, and G.J. Janz, "Fusion Properties and Heat Capacities of the Eutectic Lithium Fluoride-Sodium Fluoride-Potassium Fluoride Melt," Journal of Chemical and Engineering Data, Vol. 27, No. 3, pp. 366–367, 1982. DOI: 10.1021/je00029a041.
[23] J. Schorne-Pinto, A. Padinhare Manissery, R.E. Booth, A.C. Husek, Z. Gardiner, J. Paz Soldan Palma, J.A. Yingling, and T.M. Besmann, "Methodology for Highly Accurate Specific Heat Measurements for Molten Salts: Examples for FLiNaK and NaCl–MgCl2," International Journal of Thermophysics, Vol. 47, Article 133, 2026. DOI: 10.1007/s10765-026-03805-8.
[24] X.-H. An, J.-H. Cheng, H.-Q. Yin, L.-D. Xie, and P. Zhang, "Thermal Conductivity of High Temperature Fluoride Molten Salt Determined by Laser Flash Technique," International Journal of Heat and Mass Transfer, Vol. 90, pp. 872–877, 2015. DOI: 10.1016/j.ijheatmasstransfer.2015.07.042.
[25] S.I. Cohen and T.N. Jones, "A Summary of Density Measurements on Molten Fluoride Mixtures and a Correlation for Predicting Densities of Fluoride Mixtures," ORNL-1702, Oak Ridge National Laboratory, Oak Ridge, TN, 1954. DOI: 10.2172/4334794.
[26] T. Karlsson, M. Kropp, N. Erfurth et al., "Investigations into the Ternary NaF–KF–UF4 Salt System – Phase A," Idaho National Laboratory, Idaho Falls, ID, 2025. DOI: 10.2172/2507327.
[27] M. Fache, L. Voigt, J.-Y. Colle, J. Hald, and O. Beneš, "Thermophysical Properties of FUNaK Eutectics," Materials, Vol. 17, No. 11, Article 2776, 2024. DOI: 10.3390/ma17112776.
[28] N. Termini, R. Chesser, B. McNamara, J. Park, A. Lines et al., "Completion of Transport Property Measurements on Multiple Actinide Fluoride Mixtures," ORNL/TM-2025/4057, Oak Ridge National Laboratory, Oak Ridge, TN, 2025. DOI: 10.2172/3002248.
[29] W.D. Powers and G.C. Blalock, "Enthalpies and Heat Capacity of Solid and Molten Salt Fluoride Mixtures," ORNL-1956, Oak Ridge National Laboratory, Oak Ridge, TN, 1956. DOI: 10.2172/4794927.
[30] W.D. Powers, S.I. Cohen, and N.D. Greene, "Physical Properties of Molten Reactor Fuels and Coolants," Nuclear Science and Engineering, Vol. 17, No. 2, pp. 200–211, 1963. DOI: 10.13182/NSE63-5.
[31] R.W. Huber, E.V. Potter, and H.W. St. Clair, "Electrical Conductivity and Density of Fused Binary Mixtures of Magnesium Chloride and Other Chlorides," Report of Investigations 4858, U.S. Bureau of Mines, Washington, DC, 1952.
[32] C. Villada, W. Ding, A. Bonk et al., "Engineering Molten MgCl2–KCl–NaCl Salt for High-Temperature Thermal Energy Storage: Review on Salt Properties and Corrosion Control Strategies," Solar Energy Materials and Solar Cells, Vol. 232, Article 111344, 2021. DOI: 10.1016/j.solmat.2021.111344.
[33] M. del Rocio Rodriguez-Laguna, M.E. Woods, R. Gakhar, and A.N. Williams, "Evaluation of Bubbler Sensors for In Situ Measurement of Density, Liquid Depth, and Surface Tension in Molten Salts," Chemical Engineering

Journal Advances, Vol. 26, Article 101215, 2026. DOI: 10.1016/j.ceja.2026.101215.
[34] X. Xu, X. Wang, P. Li, Y. Li et al., "Experimental Test of Properties of KCl–MgCl2 Eutectic Molten Salt for Heat Transfer and Thermal Storage Fluid in Concentrated Solar Power Systems," Journal of Solar Energy Engineering, Vol. 140, No. 5, Article 051011, 2018. DOI: 10.1115/1.4040065.
[35] J. Lu, S. Yang, Z. Rong, G. Pan, J. Ding, S. Liu, X. Wei, W. Wang et al., "Thermal Properties of KCl–MgCl2 Eutectic Salt for High-Temperature Heat Transfer and Thermal Storage System," Solar Energy Materials and Solar Cells, Vol. 228, Article 111130, 2021. DOI: 10.1016/j.solmat.2021.111130.
[36] X. Wang, J. Rincon, P. Li, Y. Zhao, and J. Vidal, "Thermophysical Properties Experimentally Tested for NaCl-KCl-MgCl2 Eutectic Molten Salt as a Next Generation High Temperature HTF in CSP Systems," Journal of Solar Energy Engineering, Vol. 143, No. 4, Article 041005, 2021. DOI: 10.1115/1.4049253.